Supplementary materials for "scAClc: A Multi-Objective Adaptive Clustering Framework for Single-Cell Transcriptomics via Contrastive and Resolution-Aware Representation Learning"

SupplementaryTables

Table S1. The statistics of 15 real scRNA-seq datasets.

No.	dataset	organ	platform	cell types	cells	gene number
1	Human_PBMC[1]	Human PBMC	10X	8	4271	16653
2	Human_p[2]	Human pancreas	inDrop	14	3605	20125
3	Human_k[3]	kidney	10X	11	5685	25215
4	Mouse_E[4]	Mouse embryo stem cells	inDrop	4	2717	24047
5	Mouse_k[5]	Kidney	Drop-seq	8	3660	23797
6	Mouse_h[6]	Mouse brain	Drop-seq	46	12089	23284
7	Turtle_b[7]	Turtle brain	Drop-seq	15	18664	23500
8	Bach[8]	Mammary Gland	10x Genomic	8	23184	19965
9	Muraro[9]	Pancreas	CEL-seq2	9	2122	19046
10	Plasschaert[10]	Trachea	inDrop	8	6977	28205
11	Pollen[11]	Human tissues	SMARTer	11	301	21721
12	Qx_Limb_Muscle[12]	Limb Muscle	10X	6	3909	23341
13	QS_Diaphragm[12]	Diaphragm	Smart-seq2	5	870	23341
14	QS_Limb_Muscle[12]	Limb Muscle	Smart-seq2	6	1090	23341
15	QS_Lung[12]	Lung	Smart-seq2	11	1676	23341

Table S2. Clustering performance comparison of the different clustering algorithms on 15 real scRNA-seq datasets measured by ARI.

Dataset	scAClc	scMGCA	scTAG	scDFN	scDeepCluster	scSCC
Human_PBMC	**0.7813**	0.6666	0.5882	0.7704	0.7056	0.7057
Human_p	**0.9550**	0.9024	0.6954	0.6298	0.5867	0.7406
Human_k	0.6619	**0.7673**	0.6720	0.5758	0.4640	0.5695
Mouse_E	**0.9108**	0.6920	0.6711	0.7480	0.6607	0.7406
Mouse_k	**0.9349**	0.7119	0.8511	0.6525	0.7381	0.7553
Mouse_h	**0.7880**	0.4424	0.5799	0.6364	0.5314	0.3430
Turtle_b	**0.8926**	0.4858	0.5590	0.4128	0.4653	0.7658
Bach	0.8429	0.8926	0.8852	0.8524	0.5284	**0.9308**
Muraro	**0.9288**	0.8843	0.7946	0.9280	0.6372	0.9003
Plasschaert	**0.9125**	0.8215	0.5347	0.5337	0.2805	0.7465
Pollen	0.8952	0.8642	0.7538	**0.9351**	0.8220	0.7317
Qx_Limb_Muscle	0.8580	0.8090	**0.9646**	0.8011	0.4759	0.8105
QS_Diaphragm	0.9538	**0.9652**	0.9153	0.9580	0.6561	0.4645
QS_Limb_Muscle	0.9105	0.9751	0.9667	**0.9779**	0.6925	0.9559
QS_Lung	0.6138	0.5834	0.6734	0.5961	0.4101	**0.8304**
Average	**0.8560**	0.7642	0.7403	0.7339	0.5770	0.7327

Table S3. Clustering performance comparison of the different clustering algorithms on 15 real scRNA-seq datasets measured by NMI.

Dataset	scAClc	scMGCA	scTAG	scDFN	scDeepCluster	scSCC
Human_PBMC	**0.7989**	0.7473	0.6538	0.7697	0.7612	0.7466
Human_p	**0.9109**	0.8514	0.7525	0.8160	0.7723	0.7177
Human_k	0.7748	**0.8196**	0.7802	0.7400	0.6919	0.7641
Mouse_E	**0.9154**	0.6898	0.6877	0.7295	0.7480	0.7177
Mouse_k	**0.9153**	0.7949	0.8328	0.7679	0.7962	0.8363
Mouse_h	**0.7810**	0.7266	0.7382	0.7582	0.7488	0.7219
Turtle_b	**0.8628**	0.7064	0.6972	0.7175	0.7411	0.7843
Bach	0.8415	0.8338	0.8514	0.8505	0.7280	**0.8966**
Muraro	0.8847	0.8358	0.8047	**0.8924**	0.7905	0.8563
Plasschaert	**0.8618**	0.7602	0.5770	0.6836	0.5452	0.7528
Pollen	**0.9339**	0.9166	0.8606	0.9299	0.9020	0.8067
Qx_Limb_Muscle	0.9265	0.8677	**0.9470**	0.8728	0.7721	0.8874
QS_Diaphragm	0.9126	0.9392	0.8987	**0.9448**	0.8027	0.6494
QS_Limb_Muscle	0.8599	0.9568	0.9448	**0.9614**	0.8153	0.9190
QS_Lung	0.7629	0.7650	0.7996	0.7626	0.6970	**0.8215**
Average	**0.8629**	0.8141	0.7884	0.8131	0.7542	0.7919

Table S4. The number of cells on the Mouse_h dataset and the correspondence between real cell type and cell number.

Cell type	Cluster number	Cell number
Glu1	0	13
Glu2	1	21
Glu3	2	13
Glu4	3	131
Glu5	4	200
Glu6	5	51
Glu7	6	211
Glu8	7	50
Glu9	8	35
Glu10	9	15
Glu11	10	42
Glu12	11	24
Glu13	12	24
Glu14	13	51
Glu15	14	25
GABA1	15	23
GABA2	16	27
GABA3	17	97
GABA4	18	18
GABA5	19	73
GABA6	20	49
GABA7	21	17
GABA8	22	402
GABA9	23	71
GABA10	24	23
GABA11	25	35
GABA12	26	62
GABA13	27	165
GABA14	28	71
GABA15	29	112
GABA16	30	66
GABA17	31	50
GABA18	32	31
Hista	33	17
POPC	34	51
OPC	35	1741
IMO	36	151
MO	37	3541
Astro	38	1148
Ependy	39	413
Tany	40	609
Epith1	41	818
Epith2	42	379
Micro	43	724
Macro	44	167

Table S5. Clustering result comparison of scAClc in different module ((i) only HVGs; (ii) only RFGs; (iii) without the hierarchical gene relevance module; (iv) with the hierarchical gene relevance module (scAClc)) measured by ARI.

Dataset	only HVGs	only RFGs	without	scAClc
Human_PBMC	0.7344	0.7141	0.5766	0.7813
Human_p	0.9554	0.8934	0.8973	0.9550
Human_k	0.7194	0.6166	0.6778	0.6619
Mouse_E	0.8075	0.9123	0.8278	0.9108
Mouse_k	0.8141	0.7929	0.8034	0.9349
Mouse_h	0.6557	0.7733	0.8511	0.7880
Turtle_b	0.6935	0.7796	0.7663	0.8926
Bach	0.8419	0.8506	0.7724	0.8429
Muraro	0.9328	0.9331	0.7290	0.9288
Plasschaert	0.7544	0.7651	0.9361	0.9125
Pollen	0.8567	0.8656	0.3177	0.8952
Qx_Limb_Muscle	0.9933	0.9858	0.9914	0.8580
QS_Diaphragm	0.9822	0.9519	0.5874	0.9538
QS_Limb_Muscle	0.7026	0.8068	0.6400	0.9105
QS_Lung	0.9011	0.5886	0.5775	0.6138
Average	**0.8230**	**0.8153**	**0.7301**	**0.8560**

Table S6. Clustering result comparison of scAClc in different module ((i) only HVGs; (ii) only RFGs; (iii) without the hierarchical gene relevance module; (iv) with the hierarchical gene relevance module (scAClc)) measured by NMI.

Dataset	only HVGs	only RFGs	without	scAClc
Human_PBMC	0.7699	0.7656	0.7018	0.7989
Human_p	0.9127	0.8702	0.8777	0.9109
Human_k	0.8096	0.7489	0.7875	0.7748
Mouse_E	0.8271	0.916	0.8614	0.9154
Mouse_k	0.8698	0.8484	0.8600	0.9153
Mouse_h	0.6904	0.7652	0.7962	0.7810
Turtle_b	0.7428	0.8305	0.7590	0.8628
Bach	0.8522	0.8424	0.7794	0.8415
Muraro	0.8902	0.8904	0.8282	0.8847
Plasschaert	0.7550	0.7714	0.8713	0.8618
Pollen	0.9232	0.9078	0.5801	0.9339
Qx_Limb_Muscle	0.9871	0.9770	0.9840	0.9265
QS_Diaphragm	0.9686	0.9067	0.8032	0.9126
QS_Limb_Muscle	0.7666	0.7538	0.7853	0.8599
QS_Lung	0.8521	0.7290	0.7720	0.7629
Average	**0.8412**	**0.8349**	**0.8032**	**0.8629**

Table S7. Clustering result comparison of scAClc in different module ((i) standard contrastive learning; (ii) without contrastive learning; (iii) anchor-centered contrastive learning) measured by ARI.

Dataset	standard	without	anchor-centered
Human_PBMC	0.7649	0.7787	0.7813
Human_p	0.9545	0.9577	0.9550
Human_k	0.6310	0.5178	0.6619
Mouse_E	0.9123	0.9170	0.9108
Mouse_k	0.8159	0.9389	0.9349
Mouse_h	0.8269	0.5490	0.7880
Turtle_b	0.7640	0.8651	0.8926
Bach	0.8176	0.6332	0.8429
Muraro	0.9309	0.9288	0.9288
Plasschaert	0.7872	0.9110	0.9125
Pollen	0.7756	0.8951	0.8952
Qx_Limb_Muscle	0.9917	0.9903	0.8580
QS_Diaphragm	0.9783	0.9574	0.9538
QS_Limb_Muscle	0.9211	0.9171	0.9105
QS_Lung	0.7414	0.5235	0.6138
Average	**0.8409**	**0.8187**	**0.8560**

Table S8. Clustering result comparison of scAClc in different module ((i) standard contrastive learning; (ii) without contrastive learning; (iii) anchor-centered contrastive learning) measured by NMI

Dataset	standard	without	anchor-centered
Human_PBMC	0.7877	0.7966	0.7989
Human_p	0.9095	0.9138	0.9109
Human_k	0.7468	0.6869	0.7748
Mouse_E	0.9173	0.9260	0.9154
Mouse_k	0.8712	0.9189	0.9153
Mouse_h	0.8028	0.6551	0.7810
Turtle_b	0.8270	0.8345	0.8628
Bach	0.8165	0.7088	0.8415
Muraro	0.8864	0.8846	0.8847
Plasschaert	0.7786	0.8594	0.8618
Pollen	0.8960	0.9339	0.9339
Qx_Limb_Muscle	0.9845	0.9817	0.9265
QS_Diaphragm	0.9528	0.9188	0.9126
QS_Limb_Muscle	0.8641	0.8654	0.8599
QS_Lung	0.7810	0.7508	0.7629
Average	**0.8548**	**0.8423**	**0.8629**

Table S9. Clustering result comparison of scAClc in different parameters ((i) The HVG and RFG methods screen 2000 genes respectively; (ii) The HVG and RFG methods screen 3000 genes respectively; (iii) The HVG and RFG methods screen 4000 genes respectively) measured by ARI.

Dataset	2000	3000	4000
Human_PBMC	0.7544	0.7813	0.8089
Human_p	0.9559	0.9550	0.8939
Human_k	0.6413	0.6619	0.6805
Mouse_E	0.9111	0.9108	0.8222
Mouse_k	0.8129	0.9349	0.8588
Mouse_h	0.7854	0.7880	0.7875
Turtle_b	0.7682	0.8926	0.7717
Bach	0.5772	0.8429	0.6132
Muraro	0.9316	0.9288	0.7345
Plasschaert	0.9126	0.9125	0.5971
Pollen	0.7686	0.8952	0.5967
Qx_Limb_Muscle	0.9851	0.8580	0.9913
QS_Diaphragm	0.5962	0.9538	0.9682
QS_Limb_Muscle	0.9273	0.9105	0.8408
QS_Lung	0.5149	0.6138	0.7511
Average	**0.7895**	**0.8560**	**0.7811**

Table S10. Clustering result comparison of scAClc in different parameters ((i) The HVG and RFG methods screen 2000 genes respectively; (ii) The HVG and RFG methods screen 3000 genes respectively; (iii) The HVG and RFG methods screen 4000 genes respectively) measured by NMI.

Dataset	2000	3000	4000
Human_PBMC	0.7877	0.7989	0.8036
Human_p	0.9121	0.9109	0.8719
Human_k	0.7672	0.7748	0.7979
Mouse_E	0.9134	0.9154	0.8505
Mouse_k	0.8634	0.9153	0.8763
Mouse_h	0.7736	0.7810	0.7825
Turtle_b	0.7495	0.8628	0.7388
Bach	0.7404	0.8415	0.7073
Muraro	0.8882	0.8847	0.8326
Plasschaert	0.8596	0.8618	0.6915
Pollen	0.8834	0.9339	0.8039
Qx_Limb_Muscle	0.9747	0.9265	0.9844
QS_Diaphragm	0.7923	0.9126	0.9339
QS_Limb_Muscle	0.8740	0.8599	0.8313
QS_Lung	0.7581	0.7629	0.7895
Average	**0.8358**	**0.8629**	**0.8197**

Table S11. Clustering result comparison of scAClc in different parameters ((i) The contrastive-loss weight ranges from 0.10 to 0.06; (ii) The contrastive-loss weight ranges from 0.12 to 0.08; (iii) The contrastive-loss weight ranges from 0.14 to 0.10) measured by ARI.

Dataset	0.10-0.06	0.12-0.08	0.14-0.10
Human_PBMC	0.7745	0.7813	0.7791
Human_p	0.9564	0.9550	0.9559
Human_k	0.5714	0.6619	0.6629
Mouse_E	0.9150	0.9108	0.9106
Mouse_k	0.9413	0.9349	0.9349
Mouse_h	0.8309	0.7880	0.7753
Turtle_b	0.8310	0.8926	0.7951
Bach	0.6340	0.8429	0.8537
Muraro	0.9272	0.9288	0.7288
Plasschaert	0.9115	0.9125	0.6161
Pollen	0.8951	0.8952	0.8951
Qx_Limb_Muscle	0.8552	0.8580	0.9897
QS_Diaphragm	0.9538	0.9538	0.5857
QS_Limb_Muscle	0.9025	0.9105	0.9096
QS_Lung	0.7411	0.6138	0.6162
Average	**0.8427**	**0.8560**	**0.8006**

Table S12. Clustering result comparison of scAClc in different parameters ((i) The contrastive-loss weight ranges from 0.10 to 0.06; (ii) The contrastive-loss weight ranges from 0.12 to 0.08; (iii) The contrastive-loss weight ranges from 0.14 to 0.10) measured by NMI.

| Dataset	0.10-0.06	0.12-0.08	0.14-0.10
Human_PBMC	0.7954	0.7989	0.7949
Human_p	0.9122	0.9109	0.9110
Human_k	0.7251	0.7748	0.7737
Mouse_E	0.9222	0.9154	0.9150
Mouse_k	0.9217	0.9153	0.9165
Mouse_h	0.8055	0.7810	0.7634
Turtle_b	0.8017	0.8628	0.8249
Bach	0.7104	0.8415	0.8446
Muraro	0.8835	0.8847	0.8277
Plasschaert	0.8595	0.8618	0.6991
Pollen	0.9339	0.9339	0.9339
Qx_Limb_Muscle	0.9283	0.9265	0.9824
QS_Diaphragm	0.9125	0.9126	0.7686
QS_Limb_Muscle	0.8518	0.8599	0.8618
QS_Lung	0.7788	0.7629	0.7645
Average	**0.8495**	**0.8629**	**0.8388**

Supplementary Figure
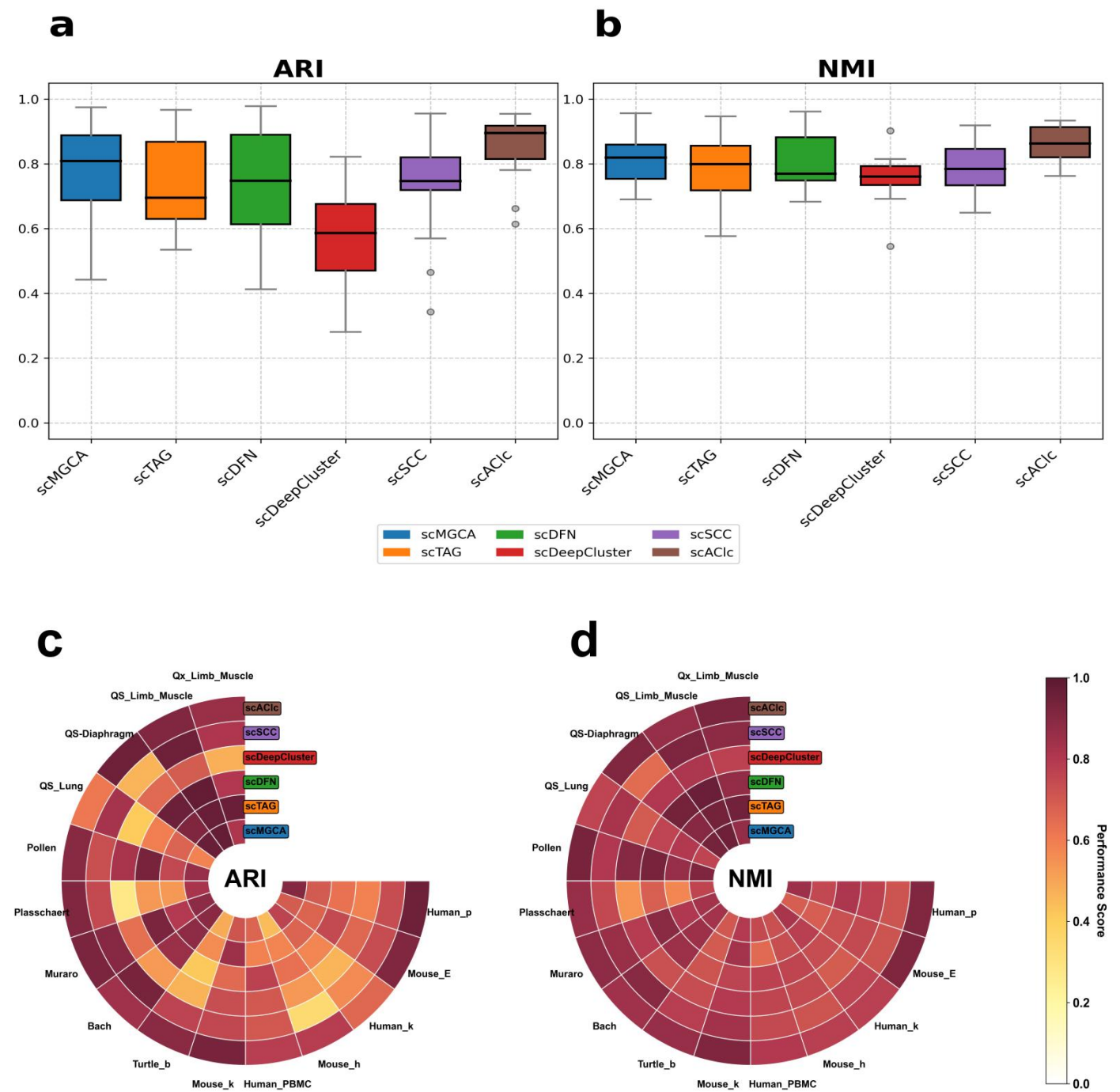
Figure S1: (a and b) A comparison of the average value of ARI and NMI on the 15 real scRNA-seq datasets among 6 clustering methods. (c and d) Specific numerical values for each method on each dataset.

Reference

[1] G. X. Zheng, J. M. Terry, P. Belgrader, P. Ryvkin, Z. W. Bent, R. Wilson, S. B. Ziraldo, T. D. Wheeler, G. P. McDermott, J. Zhu et al., "Massively parallel digital transcriptional profiling of single cells," Nature communications, vol. 8, no. 1, p. 14049, 2017.

[2] M. Baron, A. Veres, S. L. Wolock, A. L. Faust, R. Gaujoux, A. Vetere, J. H. Ryu, B. K. Wagner, S. S. Shen-Orr, A. M. Klein et al., "A single-cell transcriptomic map of the human and mouse pancreas reveals inter-and intra-cell population structure," Cell systems, vol. 3, no. 4, pp. 346–360, 2016.

[3] M. D. Young, T. J. Mitchell, F. A. Vieira Braga, M. G. Tran, B. J. Stewart, J. R. Ferdinand, G. Collord, R. A. Botting, D.-M. Popescu, K. W. Loudon et al., "Single-cell transcriptomes from human kidneys reveal the cellular identity of renal tumors," science, vol. 361, no. 6402, pp. 594–599, 2018.

[4] A. M. Klein, L. Mazutis, I. Akartuna, N. Tallapragada, A. Veres, V. Li, L. Peshkin, D. A. Weitz, and M. W. Kirschner, "Droplet barcoding for single-cell transcriptomics applied to embryonic stem cells," Cell, vol. 161, no. 5, pp. 1187–1201, 2015.

[5] M. Adam, A. S. Potter, and S. S. Potter, "Psychrophilic proteases dramatically reduce single-cell rna-seq artifacts: a molecular atlas of kidney development," Development, vol. 144, no. 19, pp. 3625–3632, 2017.

[6] R. Chen, X. Wu, L. Jiang, and Y. Zhang, "Single-cell rna-seq reveals hypothalamic cell diversity," Cell reports, vol. 18, no. 13, pp. 3227–3241, 2017.

[7] M. A. Tosches, T. M. Yamawaki, R. K. Naumann, A. A. Jacobi, G. Tushev, and G. Laurent, "Evolution of pallium, hippocampus, and cortical cell types revealed by single-cell transcriptomics in reptiles," Science, vol. 360, no. 6391, pp. 881– 888, 2018.

[8] Bach K, Pensa S, Grzelak M, Hadfield J, Adams DJ, Marioni JC, et al. Differentiation dynamics of mammary epithelial cells revealed by single-cell RNA sequencing.

[9] M. J. Muraro, G. Dharmadhikari, D. Grün, N. Groen, T. Dielen, E. Jansen, L. Van Gurp, M. A. Engelse, F. Carlotti, E. J. De Koning et al., "A single-cell transcriptome atlas of the human pancreas," Cell systems, vol. 3, no. 4, pp. 385–394, 2016.

[10] Plasschaert LW, Zilionis R, Choo-Wing R, Savova V, Knehr J, Roma G, et al. A ˇsingle-cell atlas of the airway epithelium reveals the CFTR-rich pulmonary ionocyte. Nature 2018; 560(7718): 377.

[11] A. A. Pollen, T. J. Nowakowski, J. Shuga, X. Wang, A. A. Leyrat, J. H. Lui, N. Li, L. Szpankowski, B. Fowler, P. Chen et al., "Low-coverage single-cell mrna sequencing reveals cellular heterogeneity and activated signaling pathways in developing cerebral cortex," Nature biotechnology, vol. 32, no. 10, pp. 1053– 1058, 2014.

[12] Schaum N, Karkanias J, Neff NF, May AP, Quake SR, Wyss-Coray T, et al. Single cell transcriptomics of 20 mouse organs creates a Tabula Muris: The Tabula Muris Consortium. Nature 2018; 562(7727): 367.